PASJ: Publ. Astron. Soc. Japan **49**, 101–107 (1997)

Expanding Atmosphere of the M-Type Supergiant in VV Cephei

Shusaku KAWABATA
Kyoto Gakuen University, Kameoka, Kyoto 621
and
Mamoru SAITŌ
Department of Astronomy, Faculty of Science, Kyoto University, Sakyo-ku, Kyoto 606-01

(Received 1996 August 5; accepted 1996 December 2)

Abstract

A search and radial-velocity measurements of forbidden lines were performed on spectrograms of VV Cep at 0.35–0.45 μm taken between 1976 and 1984, which was about half the orbital period around the last eclipse. We identified 13 [Fe II] lines, 3 [Ni II] lines, and one [Cu II] line including at least six new lines on the spectra of VV Cep. The radial velocities of these forbidden lines were independent of the eclipse phase, and differed with respect to the transition probability and excitation potential. The forbidden-line features indicate the presence of gaseous motions expanding from the M-type supergiant with velocities of ~ 20 km s^{-1}. The mass-loss rate is estimated to be on the order of 10^{-6} $M_\odot$ yr^{-1}.

Key words: Stars: atmospheres — Stars: eclipsing binaries — Stars: emission-line — Stars: individual(VV Cephei) — Stars: mass loss

1. Introduction

VV Cephei is a long-period (20.4 yr) eclipsing binary consisting of an M-type supergiant and a B-type companion. This binary has been known to be a massive system with outstanding spectral features of strong Balmer emissions and [Fe II] emission lines. Similar supergiant binary systems having such spectroscopic characters have been distinguished as VV Cep stars (Bidelman 1954; Cowley 1969). The Balmer emissions give clues to the structure of the B star's envelope and mass flow between the components (e.g., Wright 1977; Saijo 1981). The [Fe II] lines have been considered to originate in the circumbinary nebula because of their radial velocities around the systemic velocity (e.g., McLaughlin 1934; Peery 1966).

The last eclipse of VV Cep occurred between 1976 and 1978; during and around this eclipse many observations were performed photometrically and spectroscopically at optical and ultraviolet wavelengths, and the geometrical and physical features of the components were studied. Kawabata et al. (1981), Saijo (1981), and Möllenhoff and Schaifers (1981) confirmed the rotating envelope of the B star through an analysis of the Balmer emissions. Saitō et al. (1980) detected a 116-day periodic light variation in the M-type component. From the ultraviolet spectra Hagen et al. (1980) found the characteristics of an atmospheric eclipse and an expanding chromosphere of the M-type supergiant.

In this study we searched for forbidden lines of VV Cep on spectrograms taken around the last eclipse, and showed the presence of expanding motions of atmospheric gas. In section 2 we identify the forbidden lines on spectrograms obtained between 1976 and 1984, and show that the radial velocities depend on the transition probability and excitation potential of the lines. In section 3 such a correlation is explained as being due to expanding gas in the atmosphere of the M-type component as well as circumbinary matter with a systemic velocity. We also estimate the mass-loss rate of the M supergiant.

2. Observations and Results

The spectrograms of VV Cep were taken for wavelengths of 3500–4500 Å at the Okayama Astrophysical Observatory between 1976 and 1984 using the coudé spectrograph of the 188 cm reflector. The dispersions were about 10.2 Å mm^{-1} and the emulsions used were Eastman Kodak 103aO and IIaO. Table 1 gives a list of the 41 spectrograms used in this study, as well as the orbital phase and effective wavelengths. The orbital phases were obtained from the time of periastron passage of JD 2438461 and the period of 7430.5 d by Wright (1977), and graded to 0.005, corresponding to 37 d, although the longest period of a series of our observations was 9 d. Of the observed phases, the totality occurred for the phases from 0.66 to 0.675, and the atmospheric (partial) eclipse occurred from 0.61 to 0.63 at ingress and from 0.7 to 0.73 at egress (e.g., Saitō et al. 1980).

The photographic densities were measured using a

Table 1. Spectroscopic observations of VV Cephei between 1976 and 1984.

Plate No.	Date	JulianDay 2440000+	Phase*	Wavelength†	Remark
C4-4726	1976 8 9	3000	0.61	3768–4404	
C4-4727	1976 8 9	3000	0.61	3618–3969	
C4-4729	1976 8 10	3001	0.61	3885–4260	
C4-4730	1976 8 10	3001	0.61	3565–4021	
C4-4732	1976 8 12	3003	0.61	4045–4325	U.E.
C4-4733	1976 8 12	3003	0.61	3618–4045	
C4-4738	1976 8 14	3005	0.61	3856–4134	
C4-4741	1976 8 14	3005	0.61	3679–3997	
C4-4745	1976 8 16	3007	0.61	3647–3997	U.E.
C4-4747	1976 8 16	3009	0.61	4132–4271	
C4-4751	1976 10 2	3054	0.62	3825–4528	
C4-4791	1976 10 11	3063	0.62	3679–4063	
C4-4906	1976 12 3	3116	0.63	3902–4466	
C4-4907	1976 12 4	3117	0.63	3565–3997	
C4-4913	1976 12 6	3119	0.63	3850–4199	
C4-5062	1977 8 21	3377	0.66	4063–4466	U.E.
C4-5064	1977 8 22	3378	0.66	4045–4427	U.E.
C4-5123	1977 10 23	3440	0.67	4005–4427	
C4-5155	1977 11 25	3473	0.675	3977–4466	
C4-5159	1977 11 28	3476	0.675	3705–4021	U.E.
C4-5257	1978 5 23	3652	0.70	4005–4466	
C4-5259	1978 5 24	3653	0.70	3705–4021	
C4-5417	1978 8 21	3742	0.71	3902–4325	
C4-5420	1978 8 22	3743	0.71	3705–4134	
C4-5425	1978 8 23	3744	0.71	3565–3930	
C4-5426	1978 8 23	3744	0.71	3856–4427	
C4-5429	1978 8 24	3745	0.71	4005–4271	
C4-5437	1978 10 17	3799	0.72	3813–4427	
C4-5438	1978 10 17	3799	0.72	3547–4045	
C4-5442	1978 10 18	3800	0.72	3813–4325	
C4-5443	1978 10 18	3800	0.72	3631–3930	
C4-5450	1978 10 19	3801	0.72	3719–4260	
C4-5454	1978 10 20	3802	0.72	3618–3997	
C4-5499	1978 11 20	3833	0.725	3618–4021	
C4-5506	1978 11 21	3834	0.725	3920–4427	
C4-5560	1978 12 18	3861	0.73	4118–4710	
C4-5829	1980 7 24	4445	0.80	4045–4476	
C4-5830	1980 7 24	4445	0.80	3815–3930	
C4-5993	1981 8 14	4831	0.86	3920–4427	
C4-6189	1981 12 10	4949	0.87	3705–4132	
C4-6998	1984 10 11	5985	0.01	3679–4143	

* Following Wright (1977).
† The range of comparison lines measured.

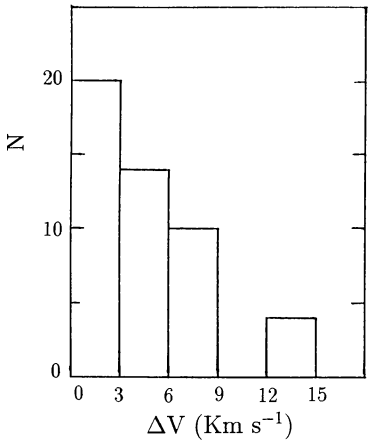

Fig. 1. Histogram of the radial-velocity differences of the same line between different spectra taken in the same phase. If three or more radial velocities were obtained for a line in the same phase, the rms values were adopted.

microdensitometer (PDS) of the Kwasan Observatory, Kyoto University. A chart of each spectrum was made in an intensity scale using a diagram processor of the Computing Center of Kyoto University.

On the spectra there are many emission-like features besides the Balmer lines. The intrinsic intensities of the two components' light are comparable to each other at around 4200 Å, and the light ratio of the B-type component to the M-type component is about 7 at 3500 Å and about 0.2 at 5000 Å (Saitō et al. 1980). For wavelengths $>$ 4000 Å, we therefore made a careful comparison of these emission-like features with the spectral atlas of a dwarf M-type star (between 3895 and 6005 Å) by Tull and Vogt (1977) and with forbidden lines in the catalogs of Moore (1959), Meinel et al. (1969), and Fuhr et al. (1988), and identified forbidden lines. For wavelengths $<$4000 Å, the VV Cep spectra were dominated by the B star's spectra; we thus examined the coincidence between the wavelengths of the emission-like features on the observed spectra and those of the cataloged forbidden lines. The 17 identified lines are listed in table 2. The equivalent widths of these lines are about 0.2 Å to 1.3 Å, and did not vary with the eclipse phase. The excitation potentials of the upper levels are from 2.83 eV to 4.73 eV for all of the lines (see table 2). Of these lines, the presence on the VV Cep spectra has been known for 7 lines of $\lambda\lambda$4244, 4276, 4287, 4319, 4359, 4413, and 4457 (McLaughlin 1934; Peery 1966). Hack et al. (1992) identified the [Ni II] line, but did not indicate the wavelength. Although the known [Fe II] line λ4416 was also identified in our search, we did not adopt this line because it is located on a strong absorption line of the M-type dwarf's spectrum. The forbidden lines of [Cu II] λ3806, [Fe II] $\lambda\lambda$4029, 4082, 4084, 4157, and 4402, and some of the three lines of [Ni II] of $\lambda\lambda$3559, 3627, and 3993 were first identified in studies of spectra of VV Cep.

We measured the radial velocities of the emission lines on the charts. The accuracy in the measurement of the wavelengths on the charts is about 0.04 Å, i.e., 3 km s^{-1} at 4000 Å. In order to estimate the accuracy of the radial-velocity measurements, we compared the radial velocities of the same line measured on different spectrograms

Table 2. Forbidden lines identified in VV Cephei and the radial velocities.

Wavelength† (Å)	Ion†	Multiplet number†	Upper level† (eV)	Transition probability† (s^{-1})	Velocity‡ V_1 (km s^{-1})	Velocity‡ V_2 (km s^{-1})
3559.86	[Ni II]	5F	3.67	4.6	−45.3±4.2	—
3627.35	[Ni II]	5F	3.60	2.8	−54.4±6.1	—
3806.34*	[Cu II]	2F	3.24		−27.8±4.3	—
3993.1	[Ni II]	4F	3.10	0.52	−16.6±4.9	−2.7 ± 7.9
4029.41*	[Fe II]	9F	3.18		−27.6±2.7	−20.0 ± 1.4
4082.0	[Fe II]	39F	4.73	0.033	−42.8±6.0	−34.0 ± 3.5
4084.32*	[Fe II]	24F	3.37		−32.8±2.8	−23.0 ± 4.5
4157.89	[Fe II]	37F	3.97	0.018	−55.1 ± 3.7	−41 :
4243.98	[Fe II]	21F	3.15	0.90	−13.2±7.4	−7.0
4244.81	[Fe II]	21F	3.22	0.25	−24.9±6.2	—
4276.83	[Fe II]	21F	3.20	0.65	−15.6±3.1	−11 :
4287.40	[Fe II]	7F	2.89	1.50	−21.0±3.1	−20.5
4319.62	[Fe II]	21F	3.22	0.53	−8.9±4.7	—
4359.34	[Fe II]	7F	2.89	1.10	−22.4±3.2	−18.0
4402.60	[Fe II]	36F	3.89	0.013	−39.9±3.0	−20 :
4413.78	[Fe II]	7F	2.89	0.81	−25.1±2.7	−20.0
4457.95	[Fe II]	6F	2.83	0.29	−19.0±2.5	−18 :

† The data are taken from Moore (1959) for the three lines with asterisk on wavelength, and from Fuhr et al. (1988) for other lines.

‡ V_1 : the mean radial velocities during the phases of 0.61 to 0.73 (see table 3), and V_2 : those during the phases of 0.80 to 0.01, where the values with error are the mean of three or four values, the values with colon are due to a single value, and the others are the mean of two values.

taken within the same phase. Figure 1 shows a histogram of the velocity differences, where for more than three measurements the rms values are given. Figure 1 indicates the uncertainty in our radial-velocity measurements of the emission lines to be about 5 km s^{-1}.

If the radial velocities of the same line were measured on two or more spectrograms in the same orbital phase, we took their mean value. The mean radial velocities are listed in table 3 for each line for each phase. The radial velocities of the metallic absorption lines were also measured on the same charts. The mean values are listed in the last row of table 3; these values are similar to the radial velocities of the metallic lines measured on the red spectrograms taken in the same orbital phase (see Kawabata et al. 1981), as well as to the radial velocities of the M star's orbital motion.

Figure 2 shows the mean radial velocities of the forbidden lines against the phase; the two curves are the velocity curves of the components by Wright (1977). The radial velocities of the forbidden lines scatter between −60 and 0 km s^{-1} from line to line. The radial velocities as well as the intensities of these emission lines were independent of the eclipse phase. The smaller number of lines shown in figure 2 for phases later than 0.8, as compared with the previous phases, are due to the relative decrease in the observed wavelength range.

For the phases of 0.61–0.73 we took the mean value of the radial velocities of each forbidden line, and give them in the second last column of table 2 as V_1 along with the rms values. If these lines are associated with the component stars, the mean velocities are only little affected by the stellar motions; this is because during this period the mean radial velocities of the components are nearly the same. It is surprising that the rms values of V_1 are comparable to or less than the uncertainty value, i.e., about 5 km s^{-1}, in our radial-velocity measurements, although V_1 ranges from −55.1 km s^{-1} to −8.9 km s^{-1}.

The radial velocities V_1 are plotted in figures 3 and 4 as functions of the transition probability and excitation potential of the upper level, respectively. The plots in figure 3 are separated into three groups. The first group consists of those lines with $A \sim 1$ s^{-1} and

Table 3. Radial velocities of forbidden lines and metallic absorption lines of VV Cephei.*

Phase	0.61	0.62	0.63	0.66	0.67	0.675	0.70	0.71	0.72	0.725	0.73	0.80	0.86	0.87	0.01
Forbidden lines															
3559.86 [Ni II]	−41:	...	−44:	...	...	...	...	−51:		...	...	...	...	...	...
3627.35 [Ni II]	−54	...	−43:	...	...	...	...	−57:	−61	−57:	...	...	...	...	...
3806.34 [Cu II]	−31	−19:	−29:	...	...	−33:	−27:	−25	−32	−26:	...	...	...		
3993.1 [Ni II]	−21	−18	−11	...	...	−17	−7:	−16	−22	−21	...	...	−5:	8:	−11:
4029.41 [Fe II]	−32	−26:	−26	...	−31:	−24	−30:	−26	−28	−25:	...	...	−19:	−22:	−19:
4082.0 [Fe II]	−52	−56:	−42	−43	−46:	−37:	−39:	−40	−41	−40:	...	−35:	−37:	−28:	−36:
4084.32 [Fe II]	−35	−36:	−33	−34	−37:	−32:	−30:	−27	−33	−31:	...	−30:	−24:	−19:	−19:
4157.89 [Fe II]	−53:	−62:	...	−58	−56:	−51:	−49:	−55	−58	−54:	...	−41:		...	...
4243.98 [Fe II]	−14	−14:	−34:	−10	−8:	−7:	−12:	−9	−15	−9:		−12:	−2:	...	...
4244.81 [Fe II]	−30			−28	−30:	−23:		−22	−24	−11:				...	...
4276.83 [Fe II]	−20	−17:	−15:	−14	−16:	−13:	−15:	−21:	−18	−10:	−13:	−11:		...	...
4287.40 [Fe II]	−23	−26:	−17:	−20	−22:	−15:	−24:	−22:	−22	−18:	−22:	−20:	−21:	...	...
4319.62 [Fe II]	−12	−13:		0	−4:	−7:	−14:	−6:	−14:	−13:	−6:			...	...
4359.34 [Fe II]	−23:	−26:		−22	−24:	−19:	−22:		−21:	−17:	−28:	−19:	−17:	...	...
4402.60 [Fe II]	−40:	−45:		−37	−43:	−37:	−40:		−40:	−35:	−42:		−20:	...	...
4413.78 [Fe II]	...	−26:					−25:			−20:	−30:	−21:	−19:	...	...
4457.95 [Fe II]	...	−21:	−20:	−21:	...	−15:	−16:	...	...	...	−21:	−18:	...	...	...
Metallic absorption lines	−24	−19	−20	−19	−22	−18	−22	−14	−18	−8	−22	−5	−5	1	−6

* The radial velocities with colon were obtained on a plate, while others were the mean values of those measured on two or more plates. Blanks mean that the wavelengths were in the spectral ranges but the emission lines were not clearly identified.

$V_1 \sim -20$ km s^{-1}. These velocities are nearly the same as the mean velocity of the metallic absorption lines during this period, which was -18.7 ± 4.3 km s^{-1}, and also the systemic velocity, -20.2 km s^{-1} (Wright 1977). The second group consists of three [Fe II] lines with $A \sim 10^{-2}$ s^{-1} and $V_1 \sim -50$ km s^{-1}. The third group consists of two [Ni II] lines with $A \sim 3$ s^{-1} and $V_1 \sim -50$ km s^{-1}. The three groups are also systematically separated from each other in figure 4; the excitation potentials are higher in order of the second, third, and first groups.

Among the three forbidden lines with an unknown transition probability, the lines $\lambda\lambda$3806 and 4029 belong to the first group with respect to the relation between the radial velocity and the excitation potential, and another line λ4084 seems to be intermediate between the first and second or third groups.

3. Discussion

As shown in figure 2, the radial velocities of the M star are -10 to 0 km s^{-1}, and those of the B star are -35 to -45 km s^{-1} during the orbital phases of 0.8 to 0.01. For this period the mean values of the radial velocities of the 12 forbidden lines are listed in the last column of table 2 as V_2. The values of V_2 also scatter over a large range from -34 km s^{-1} to -2.7 km s^{-1}, whose values are somewhat higher than those of V_1.

From the two radial velocities, V_1 and V_2, given in the last two columns of table 2, we find that the radial velocities of the forbidden lines in the first group increased slightly between the phases of 0.61–0.73 and 0.80–0.01; i.e., the increments are about 0.5 to 6.2 km s^{-1} for the six lines. McLaughlin (1934) identified the five first-group forbidden lines $\lambda\lambda$4244, 4277, 4287, 4414, and 4416 on the spectra taken between 1932 August and 1933 December (around 0.25 in orbital phase) before the 1936–1938 eclipse, and found nearly constant radial velocities with a mean value of -18.1 km s^{-1}. Peery (1966) obtained almost constant radail velocities of about -20 km s^{-1} for the first-group lines of 4276.87 Å and 4287.40 Å at the phases of 0.3–0.5 before the 1956–1958 eclipse. These radial velocities are nearly the same as the first-group velocities obtained in the present study. We thus confirmed that the [Fe II] lines of the first group originate at the circumbinary envelope which always appears with radial velocities similar to the systemic velocity.

For the three [Fe II] lines of the second group, which were first identified in this study and have smaller

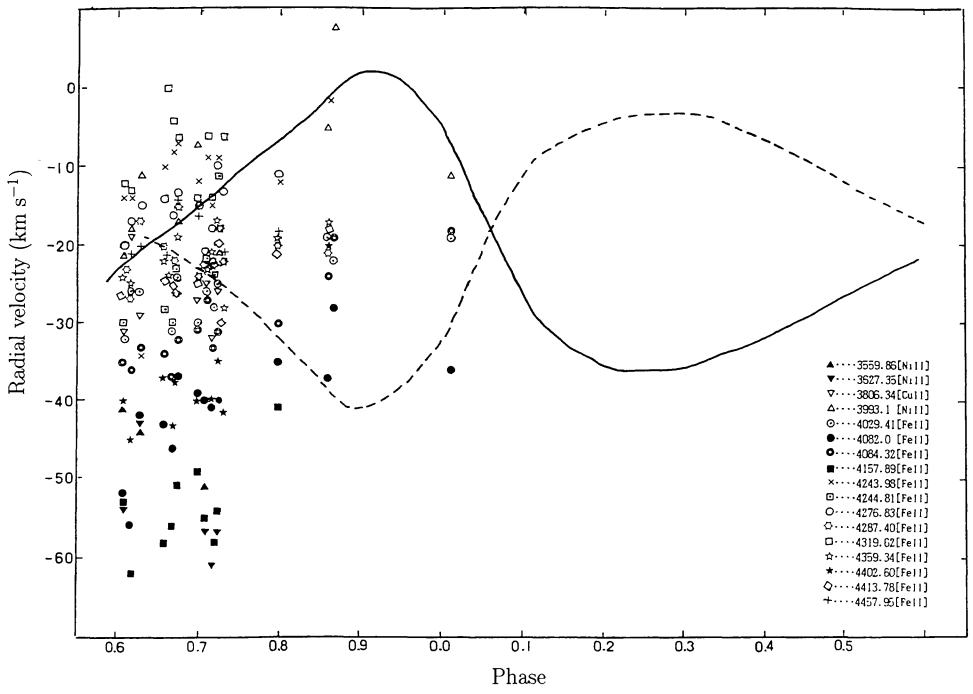

Fig. 2. Radial velocities of the forbidden lines of VV Cep as a function of the orbital phase. The radial velocities of the component stars were given by Wright (1977); the solid line denotes the M star and the dashed line the B star.

transition probabilities ($A \sim 10^{-2}$ s^{-1}) and lower radial velocities, the radial velocity increments, $V_2 - V_1$, between the phases of 0.61–0.73 and 0.80–0.01 are 8.8, 14.1, and 19.9 km s^{-1}, respectively; these values are close to the mean radial-velocity increment, 14.9 km s^{-1}, of the metallic absorption lines of the M star (see table 3). This fact implies the association of the [Fe II]-emitting gas with the M star; i.e., the atmospheric gas is expanding with radial velocities of $\sim$ 20 km s^{-1}, and the densities are about two orders of magnitude lower and the temperatures are somewhat higher than those of the circumbinary envelope emitting the first-group lines. The expanding atmosphere possibly correlates with the expanding chromosphere suggested by Hagen et al. (1980) based on the asymmetric double-peaked emission of the Mg II h and k lines.

The third group of the forbidden lines in VV Cep consists of two [Ni II] lines. They have the lowest radial velocities, similar to those of the second-group lines, and the transition probabilities larger than those of the first- and second-group lines. The excitation potentials are between those of the first and second groups. Hack et al. (1992) reported that the [Ni II] line (without wavelength) had almost constant velocities of -60 km s^{-1} throughout the phases of 0–0.2 and 0.5–1.0 between 1967 and 1981. The appearances of the [Ni II] lines on the spectrograms were due to the considerably weaker continuum intensities at 3500–3600 Å compared with those at 4200–4500 Å (Saitō et al. 1980). These lines may originate in gaseous condensations existing in the rarefied gas outflowing from the M star and emitting the second-group forbidden lines. Hagen Bauer et al. (1991) suggested based on their observations of ultraviolet absorption lines btween 1978 and 1990 the presence of gaseous clumps in the outer atmosphere of the M supergiant. Stencel et al. (1993) found the existence of short-term UV continuum variations in 1991, and interpreted as meaning that a nonuniform mass transfer from the M star to B star occurred in the form of clumps of matter with a radius of $\sim 200\ R_\odot$.

The mass-loss rate of the M-type supergiant is estimated to be $4\pi r^2 n_{\rm H} m_{\rm H} v_{\rm exp} \simeq 1 \times 10^{-14} n_{\rm H} (r/R_{\rm M})^2\ M_\odot$ yr^{-1} for an expansion velocity $v_{\rm exp}$ of 20 km s^{-1}, obtained in the present study and an radius of the M star of 1900 $R_\odot$ by Saitō et al. (1980), where $m_{\rm H}$ is the mass of the hydrogen atom and $n_{\rm H}$ and r are, respectively, the number density (cm^{-3}) and radius of the second-group [Fe II]-emitting envelope. Since the envelope is comoving with the M star, we can set $r \simeq R_{\rm M}$. The electron density in the envelope is about 3×10^6 cm^{-3} for $A \simeq 0.01$ s^{-1}, a kinetic temperature of $\sim$ 5000 K, and a cross-section of $\sim 10^{-15}$ cm^2 between the electron and ion (e.g., Osterbrock 1974). If the electrons in the envelope mostly come from singly ionized metals, $n_{\rm H}$ is about 2×10^{10} cm^{-3} for the solar abundance. The resulting mass-loss rate is $\sim 2 \times 10^{-4}\ M_\odot$ yr^{-1}. This rate is the upper limit because the expanding velocity 20 km s^{-1}

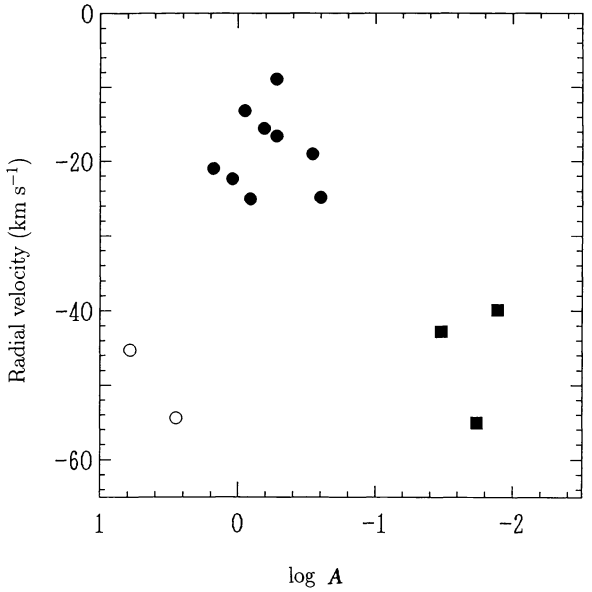

Fig. 3. Radial velocities of the forbidden lines as a function of the transition probability, A (s^{-1}). The velocities are the mean values during the phases of 0.61 to 0.73. The plots are divided into three groups: the first group is indicated by filled circles, the second by filled squares, and the third by open circles.

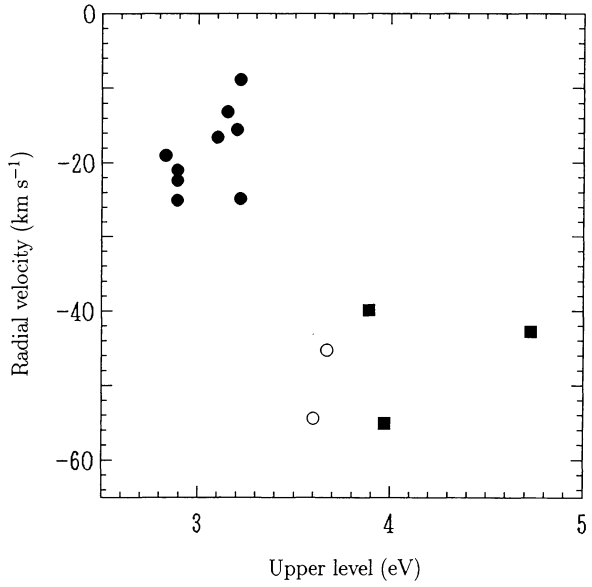

Fig. 4. Same as figure 3, but for a function of the excitation potential of the upper level of each line.

is less than the escape velocity, ~ 60 km s^{-1}, at the M star's surface with a radius of about 1900 $R_\odot$ and a mass of about 18 $M_\odot$ (Wright 1977); also, the ionization degree in the envelope may be higher than 10^{-4} used.

For $m_B = 7.28$ of the M star (Saitō et al. 1980), the photon flux of a forbidden line with an equivalent width of EW(Å) around 4400 Å is about $1 \times 10^{44}[EW(\text{Å})]D^2$ s^{-1}, where D is the distance to VV Cep in kpc. On the other hand, the photon flux from ions in a spherical layer just above the photosphere with a radial thickness of Δr and an ion density of n_i cm^{-3} is about $3 \times 10^{43} n_i A (r/R_M)^2 (\Delta r/R_M)$ s^{-1} for $R_M = 1900\ R_\odot$. For $D \simeq 0.7$ kpc from the astrometry (van de Kamp 1978) and $EW \simeq 0.3$ for the second-group [Fe II] lines with $A \sim 0.01$ s^{-1}, the two expressions for the photon-flux yields the equation $n_i(\Delta r/R_M) \sim 40$ cm^{-3}, where the radial thickness Δr may be taken as $\Delta r \simeq (0.1\text{–}0.3)R_M$ because the electron densities are nearly constant in the envelope. We thus have $n_i \simeq 100$–400 cm^{-3}. If we take n_i to be a tenth of the total number density of Fe atoms and ions, based on the number of observed forbidden lines with $A \sim 0.01$ s^{-1}, we obtain $n_H \simeq 10^{7.4}$–$10^{8.0}$ cm^{-3} for the solar abundance, $n(\text{Fe})/n(\text{H}) = 10^{-4.4}$. The hydrogen densities are comparable to a lower-limit value of $n_H \sim 10^8$ cm^{-3}, derived by Hagen et al. (1980) for the envelope of the M star emitting fluorescent Fe II emissions. The hydrogen density yields a mass-loss rate two or three orders of magnitude less than the upper limit obtained above, and also gives an ionization degree of ~ 0.01–0.1. Thus, the mass-loss rate of the M-type supergiant of VV Cep is on the order of $10^{-6}\ M_\odot$ yr^{-1}. The mass-loss rate is nearly equal to that estimated by Stencel et al. (1993) from a short-time scale variation of UV continuum of the B star due to obscuration by infalling matter from the M star. The rate is also consistent with the value $\sim 4 \times 10^{-6}\ M_\odot$ yr^{-1} derived by an emprical relation of Reimers (1975) for $M = 18\ M_\odot$, $R = 1900\ R_\odot$, and $L = 10^5\ L_\odot$.

We would like to thank H. Maehara, K. Saijo, and H. Sato for their help of the observations at Okayama. We also thank the referee for valuable comments.

References

Bidelman W.P. 1954, ApJS 1, 175
Cowley A.P. 1969, PASP 81, 297
Fuhr J.R., Martin G.A., Wiese W.L. 1988, J. Phys. Chem. Ref. Data 17, Suppl. No.4
Hack M., Engin S., Yilmaz N., Sedmak G., Rusconi L., Boehm C. 1992, A&AS 95, 589
Hagen W., Black J.H., Dupree A.K., Holm A.V. 1980, ApJ 238, 203
Hagen Bauer W., Stencel R.E., Neff D.H. 1991, A&AS 90, 175
Kawabata S., Saijo K., Sato H., Saitō M. 1981, PASJ 33, 177
McLaughlin D.B. 1934, ApJ 79, 380
Meinel A.B., Aveni A.F., Stockton M.W. 1969, Catalog of Emission Lines in Astrophysical Objects (University of Arizona, Tucson)
Möllenhoff C., Schaifers K. 1981, A&A 94, 333
Moore C.E. 1959, A Multiplet Table of Astrophysical Interest (U.S. Department of Commerce, Washington D.C.)

Osterbrock D.E. 1974, Astrophysics of Gaseous Nebulae (W.H. Freeman and Company, San Francisco) p45
Peery B.F. Jr 1966, ApJ 144, 672
Reimers D. 1975, in Problems in Stellar Atmospheres and Envelopes, ed B. Baschek, W.H. Kegel, G. Traving (Springer-Verlag, Berlin) p229
Saijo K. 1981, PASJ 33, 351
Saitō M., Sato H., Saijo K., Hayasaka T. 1980, PASJ 32, 163
Stencel R.E., Potter D.E., Bauer W.H. 1993, PASP 105, 45
Tull R.G., Vogt S.S. 1977, ApJS 34, 505
van de Kamp P. 1978, S&T 56, 397
Wright K.O. 1977, JRASC 71, 152